

For reprint orders, please contact: [reprints@futuremedicine.com](mailto:reprints@futuremedicine.com)

# Single-molecule force spectroscopy: a method for quantitative analysis of ligand–receptor interactions

The quantitative analysis of molecular interactions is of high interest in medical research. Most methods for the investigation of ligand–receptor complexes deal with huge ensembles of biomolecules, but often neglect interactions with low affinity or small subpopulations with different binding properties. Single-molecule force spectroscopy offers fascinating possibilities for the quantitative analysis of ligand–receptor interactions in a wide affinity range and the sensitivity to detect point mutations. Furthermore, this technique allows one to address questions about the related binding energy landscape. In this article, we introduce single-molecule force spectroscopy with a focus on novel developments in both data analysis and theoretical models for the technique. We also demonstrate two examples of the capabilities of this method.

**KEYWORDS:** atomic force microscopy ■ force spectroscopy ■ ligand–receptor ■ single molecule

Alexander Fuhrmann<sup>1</sup>  
& Robert Ros<sup>1\*</sup>

<sup>1</sup>Department of Physics, Arizona State University, Tempe, AZ 85287-1504, USA

\*Author for correspondence:

Tel.: +1 480 727 9280

Fax: +1 480 965 7954

[robert.ros@asu.edu](mailto:robert.ros@asu.edu)

The investigation of the kinetics of ligand–receptor complexes is usually carried out in ensemble methods such as surface plasmon resonance (SPR). However, this technique is inaccurate for very low-affinity interactions [1], and is also unable to identify different binding modes of subpopulations and multivalent energy landscapes. With the advent of mechanical and optical single-molecule technologies, several techniques are available to manipulate and characterize biomolecules on the level of individual molecules (for reviews about the different techniques see [2–4]). Among these methods, the most prominent mechanical approach for the analysis of ligand–receptor interactions is based on atomic force microscopy (AFM) [5].

In an atomic force microscope, a tiny tip attached to a microfabricated cantilever can be moved in three dimensions with subnanometer accuracy. The tip is brought near the surface of the sample of interest and forces acting on the tip cause the cantilever to bend. To measure the forces, a laser beam is aimed at the top of the cantilever and reflected onto a photodiode [6]. When the cantilever bends, the beam is deflected and the signal from the photodetector changes accordingly. Calibrating the system facilitates pN-resolution measurements (FIGURE 1A) [7].

By attaching molecules of one kind to the AFM tip and another kind to the surface probed by the tip, the molecular binding forces of interest can be quantified. In single-molecule force spectroscopy (SMFS) experiments, the binding partners are immobilized on the tip and surface,

respectively, and the force acting on the tip is measured as it is cycled up and down relative to the surface. At the time the tip is close or in contact with the surface, the interacting partners can bind; retracting the tip increases the force acting on the complex, until the molecules dissociate (FIGURE 1B). The small radius of the AFM tip (~10 nm) and a careful covalent immobilization of the binding partners in very low surface densities make it possible to restrict the interactions to single molecules. Furthermore, the immobilization protocol must prevent receptor clustering.

Beginning with the pioneering work on complementary DNA strands [8], biotin–streptavidin [9,10] and cell adhesion proteoglycans [11], this method has been applied to a wide range of interactions: from complex biological ones such as antibody–antigen [12–14], protein–nucleic acid [15–19], quadruplex nucleic acids [20], enzyme–inhibitor [21] and cell adhesion molecules [22–24], to synthetic biology [25] and supramolecular examples [26]. The results of these experiments demonstrate that the technique can be applied to ligand–receptor interactions with dissociation constants,  $K_D$ , ranging from fM to  $\mu$ M with point mutant sensitivity. Several publications demonstrated the potential of this technique for affinity ranking applications [14,25,27]. With SMFS, the rate of dissociation,  $k_{off}$ , can be determined without the influence of rebinding events. Furthermore, parameters related to the binding potential are accessible, yielding information about the molecular binding mechanisms.

future  
medicine part of fsg

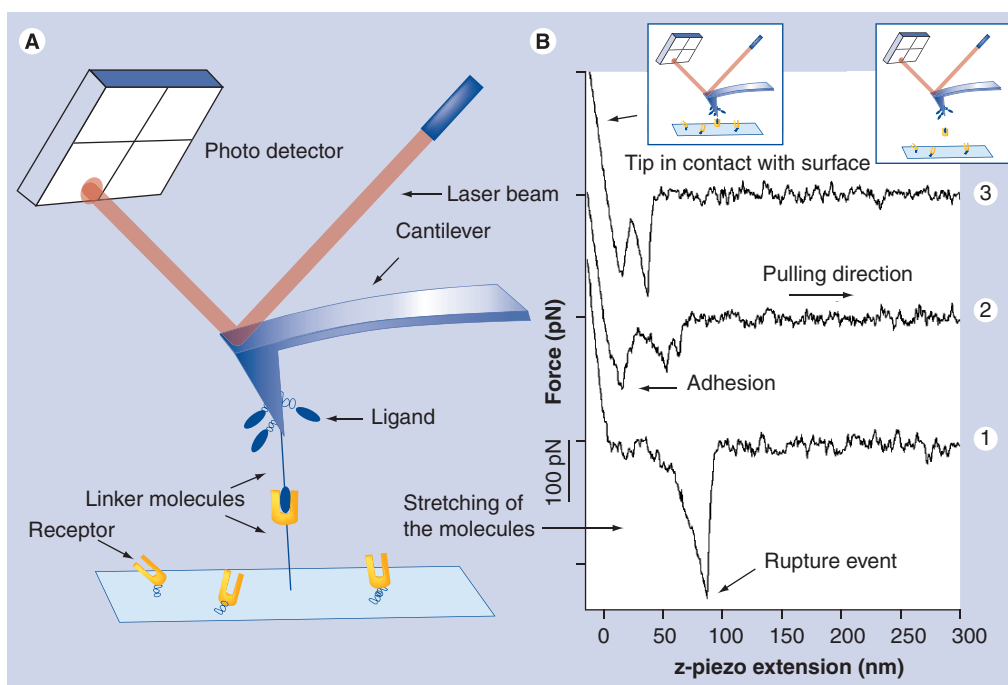


**Figure 1. Typical single-molecule force spectroscopy set-up and typical force–distance curves.** (A) Typical single-molecule force spectroscopy set-up. The atomic force microscopy tip can be moved relative to the surface with sub-nanometer precision, while forces in the pico–micro Newton range can be determined by the deflection of the cantilever. The molecules are immobilized via a linker on the tip and surface, respectively. (B) Typical force distance curves (only the retracting part) showing rupture and adhesion events. (1) A typical specific rupture force event of molecules connected via two 30-nm poly(ethylene) glycol linkers. After accounting for the movement of the cantilever due to the bending, the rupture length is 58 nm. (2) A double rupture event. Although this last event might be a single-molecule event, it should not be counted for single-molecule analysis, since the distance-dependent force is not known and cannot be reconstructed. (3) A system with a 30-nm linker on the cantilever and a 2-nm linker on the surface.

### Single-molecule force spectroscopy experiments

The immobilization of the ligand and receptor molecules on the AFM tip and sample surface, respectively, are crucial for the success of the experiments. Among the research groups performing these experiments, it is standard to use covalent chemistry to attach the molecules [28]. This ensures that the only rupture events measured are those between the receptor and the ligand, by allowing events only within the length range of the used linkers for the statistical analysis. Another important general rule is to attach the molecules to the tip and surface, respectively, using linker molecules, such as hetero-bifunctional poly(ethylene) glycols (PEG) with lengths between 10 and 40 nm. A typical immobilization set-up can be seen in FIGURE 2. Attaching each binding partner to the tip or surface with flexible linkers is crucial for three reasons: it enables the molecules to rotate freely and, thus, makes the binding site accessible; it increases the distance between the tip and surface and, thus, mitigates direct tip–surface interactions such as

electrostatics, which would otherwise influence the ligand–receptor rupture force; and it enables the discrimination of single-molecule events.

In force spectroscopy experiments, the cantilever is cycled down to the surface and then retracted. If the binding partners build a complex when the cantilever is cycled down, the cantilever bends towards the surface during retraction after the tip leaves the surface. The molecules are stretched, and the force acting on the complex increases until the bond between the ligand and receptor breaks and the cantilever jumps back to normal position. FIGURE 1B shows three typical force–distance curves (only the retracting part is shown) using different linker lengths observed in SMFS experiments. Curve 1 is acquired in an experiment using approximately 30-nm linkers on both ligand and receptor. This is an example of a curve that can be assumed to show the unbinding of a single ligand–receptor pair: there is only one rupture at a distance corresponding to the length of the two linkers. However, many curves observed in SMFS are difficult to analyze, such as 2 and 3. Curve 2 shows a double rupture

event. Such events occur when two molecules are pulled simultaneously. Although the second rupture event on the curve might correspond to the dissociation of a single complex, these data are critical because the force–extension characteristic is altered by the first rupture event. In curve 3, a ligand is attached to the tip via a 30-nm linker, while the receptor is immobilized on the sample surface by a linker only 2 nm long. The curve shows high adhesion (direct tip–surface interaction), which commonly occurs in SMFS experiments. Adhesion also alters the force–extension characteristic and, thus, these data cannot be analyzed in accordance with the theoretical models (see later). These examples demonstrate that linkers are crucial for successful SMFS experiments.

In order to gain quantitative information about the dissociation rate, it is necessary to vary the loading rate by varying the pulling velocity [29]. At very low pulling velocities, the thermal drift of the cantilever causes deviations in the determination of the forces, while at higher pulling velocities the hydrodynamic drag of the cantilever and increased noise causes deviations. Recommended pulling speeds should not exceed a few  $\mu\text{m/s}$  for standard sized cantilevers, otherwise the deviation of the deflection is too high and would require a correction in the analysis [30]. Instead of probing the sample with constant pulling velocities, it is possible to estimate the rate of dissociation and the reaction length by probing with constant pulling forces (after a certain trigger force is reached) [31]. However, this is not a common approach for AFM-based receptor–ligand experiments.

The robust detection and characterization of rupture events in the acquired force distance curves is still challenging. There are few reports that describe how (semi-)automatic software can detect such events [32–34]. Other software focuses mainly on the detection and characterization of protein unfolding events or multiple ruptures in general [35–37].

### Theory behind single-molecule force spectroscopy

The analysis and interpretation of the acquired force–distance curves is still challenging. Information regarding the strength of the molecular bond can be quantified in terms of the dissociation rate  $k_{\text{off}}$  and the reaction length  $x_b$  (i.e., the distance between potential minimum and maximum along the direction of pulling). In a breakthrough paper [29], Evans and Ritchie pioneered an analysis method based on a model by Bell [38]. The main idea is that the applied

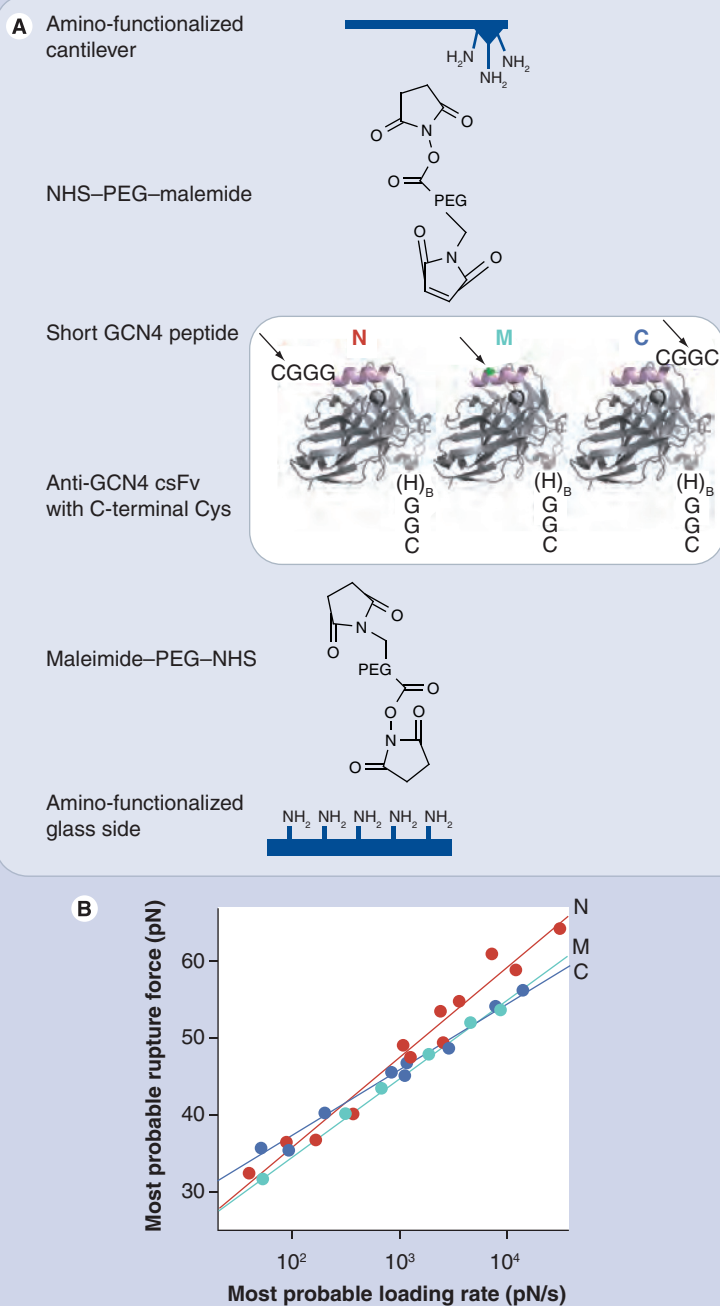


**Figure 2. Single-molecule force spectroscopy on antibody–antigen interactions.** (A) Experimental set-up of [53]. The antibody fragments are immobilized onto an amino-functionalized glass slide using a heterobifunctional PEG linker. The same procedure is used to immobilize the short antigen peptides on the cantilever. N, M and C correspond to different linker attachment configurations. In N, a cysteine and three glycine residues were attached to the N-terminus of the peptide. In M, alanine on position 8 of the peptide sequence was exchanged for cysteine. In C, three glycine residues followed by a cysteine were attached to the C-terminus of the peptide. While these changes do not affect the equilibrium dissociation rates (i.e., without external force), they change the direction of pulling. (B) The most probable rupture force plotted (semi-logarithmically) against the corresponding loading rate for all three configurations of N, M and C. By using the standard theory (see theory section) one can gain the corresponding reaction length from the slope of the fitted line and the dissociation rate from the intersection of the fitted line with the y-axis. NHS: N-hydroxysuccinimide; PEG: Poly(ethylene) glycol. Adapted from [53] with permission from Elsevier © (2008).

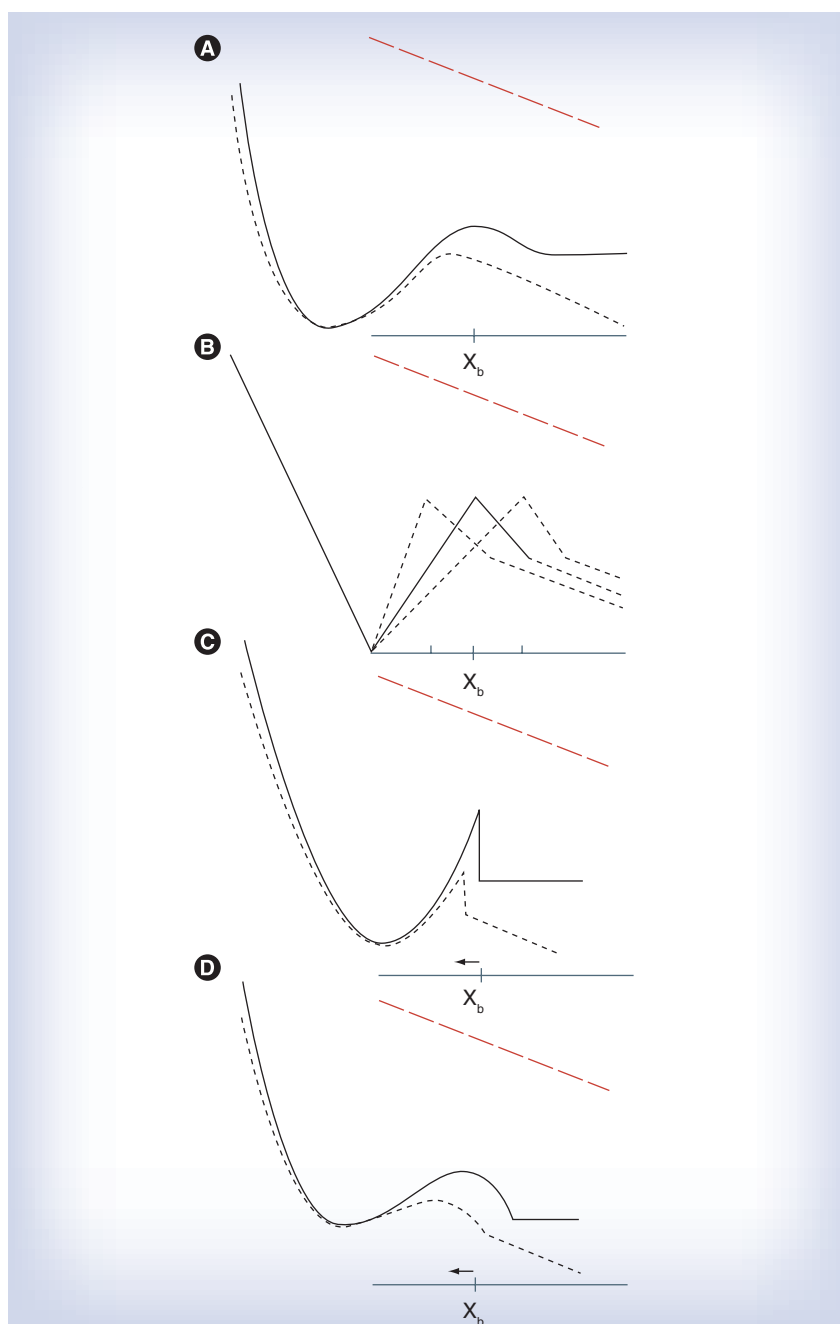


**Figure 3. Potential barriers under the influence of external force, as assumed by the various theoretical models.** The potential barriers are aligned at the potential minima. Thus, (A, C & D) appear to be shifted to the left under the external force. (A) Shape of an example potential (solid line) under influence of externally applied force (wide dashed red line). The resulting potential is tilted and shows a lower potential barrier (dashed line). (B) Shows the standard model (solid line) and heterogeneous bond model (dashed line) under the influence of an external force. The potential barrier without external force is not shown. In the standard model by Evans and Ritchie the potential barrier is assumed to be linear (solid line). In this model, the external force lowers the energy barrier but does not affect the reaction length. This would correspond to  $\nu = 1$ . The potential barrier in the heterogeneous bond model (dashed lines) has a Gaussian-distributed reaction length. The external force does not affect the mean value of this length. (C) Cusp model of the potential, corresponding to  $\nu = 1/2$  (solid line). The external force lowers the potential wall and shifts it to smaller values (dashed line). (D) Cubic model corresponding to a factor  $\nu = 2/3$ .

external force lowers the free activation barrier, increasing the probability for a thermally activated dissociation and, therefore, the dissociation rate of the complex. FIGURE 3A is an example of an energy landscape and its change under a constant external force. Evans and Ritchie assume a piecewise linear potential (FIGURE 3B, solid line) and a constant loading rate (i.e., pulling velocity  $\times$  slope of rupture curve) at each pulling velocity. The result is a convenient method to calculate  $k_{\text{off}}$  and  $x_b$ . This consists of obtaining the most probable rupture force for various pulling velocities, plotting them on a semilogarithmic scale against the loading rate and fitting a straight line to the data points (FIGURE 2). The reaction length and the thermal off-rate can then be inferred from the slope and the axis intercept. In this article, this will be referred to as ‘the standard model’.

The standard model fails to explain some of the experimental data acquired in recent years. Several of the model’s assumptions are challenged by the data. One such assumption is that the loading rate is constant with respect to pulling velocity. Since most commonly used linker molecules show a nonlinear force–extension characteristic and might also have a significant distribution in length, the model requires a correction [34,39–41]. This correction improves predictions of  $k_{\text{off}}$  by a factor of up to 8 [39]. The standard model also implies that the natural logarithm of the survival probability of the bonds,  $n(f_v)$ , is inversely proportional to the pulling velocity  $v$ , such that  $-v \times \ln(n(f_v))$  is independent of  $v$  [42]. This means that in a plot such as FIGURE 4B all points should be independent from the pulling velocity  $v$  (i.e., should collapse to a single master curve). To the authors’ best knowledge, there is no SMFS ligand–receptor experiment validating this prediction; in fact, experiments rather invalidate it [42,43]. Furthermore, the model does not accurately describe the width of the experimental force histograms: the distribution of the data is much wider than the theoretical model predicts (FIGURE 4A).

Hypotheses have been proposed to explain the deviations between standard model predictions and experimental results. One possibility is that the incorrect analysis of multiple rupture events mistakenly identified as single rupture events significantly distorts experimental results. This explanation is partly confirmed in detailed investigations of the influence of multiple rupture events [44,45]. Nevertheless, due to the experimental set-up it could not be shown clearly that multiple rupture events are the main reason for the deviation from the standard theory.

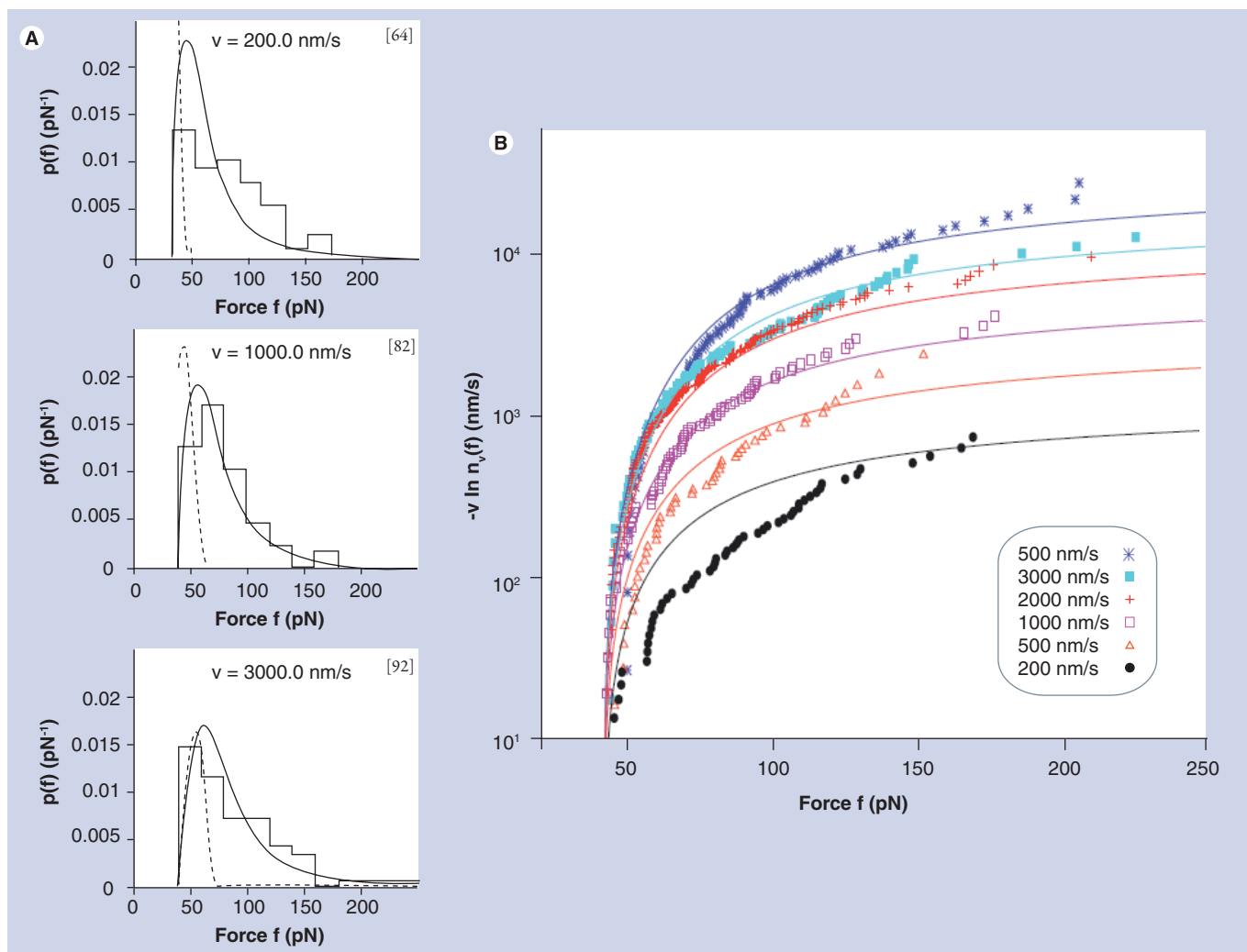


**Figure 4. Analysis of single-molecule force spectroscopy data. (A)** Rupture force histograms of selected pulling velocities of DNA–protein interactions from [15]. The number of rupture forces is indicated in brackets. Solid lines: maximum likelihood fit for the heterogeneous bond model. Dashed lines: theoretical distributions for the standard model rescaled by a factor of one-third. The distributions have been calculated by using the standard method. **(B)** The functions  $-v \times \ln(n(f, v))$  of the experimental rupture force data [15] for all pulling velocities. Each point corresponds to one observed rupture event. Solid lines: theoretical functions  $-v \times \ln(n(f, v))$  for the heterogeneous bond model.

Adapted from [34] with permission from the American Physical Society © (2008).

Interestingly, investigations of the high force regime ( $>200$  pN) indicate that multiple ruptures can be distinguished from single ruptures in this regime, due to significant differences in their force–extension characteristics [46].

Another hypothesis, termed the ‘heterogeneity of chemical bonds’ model, attributes the variations in the measured dissociation rate to a number of physical fluctuations. Among these fluctuations are changes in the local chemical environment, the orientation and structure of the molecules, multiple rupture events and non-specific binding, all of which may give rise to variations in the reaction lengths ( $x_b$ ) (compare FIGURE 3B, small dashed lines) [47]. Variations in experimental measurements of  $x_b$  are in good agreement with this model, especially after

an enhanced force curve analysis method (FIGURE 4) [34]. It should be noted that due to the rather small number of events at the lower pulling velocities (especially at 200 nm/s), deviations due to random fluctuations increase.

The previously mentioned models rely on Bell’s assumption that the (mean) reaction length does not depend on the external force. But for each realistic potential this is only true for small forces. In general, the distance between the potential minimum and maximum, and hence the dissociation length, decreases with increasing force (FIGURE 3). In more realistic models this effect should be taken into account. However, since the shape of the potential is crucial for this force–reaction length dependence, but on the other hand unknown, assumptions about the

shape have to be made [48]. For potential barriers high enough under external force that Kramer's theory is still applicable (this is a crucial assumption of the model that cannot be checked), the force-dependent dissociation rate can be written in terms of  $x_b$ ,  $k_{\text{off}}$ , a fixed exponent  $\nu$  and an additional fit parameter (i.e., the free activation barrier height). This model will be referred to as the 'extended Bell model'. The exponent  $\nu$  determines the shape of the potential barrier and its behavior under the influence of an external force (FIGURE 3C & 3D).  $\nu$  cannot be used as a fit parameter but significantly influences the estimated free activation barrier height. Thus, one will be unsure about the true shape of the energy barrier. It should be mentioned that this extended Bell model also implies the collapse of all data points in the plot of FIGURE 4 to a single curve, such that  $-\nu \times \ln(n(f_\nu))$  is independent of  $\nu$ .

The works discussed mainly focus on the theory of SMFS experiments. Researchers are left with the problem of how best to extract quantitative results from the acquired data. Accordingly, there are several works that focus on methods of finding the parameters relevant to the various models [31,39,49,50]. Getfert *et al.* came to the conclusion that a maximum likelihood estimate yields significant improvements, regardless of which model is used [51]. The advantage is that the estimation of the model parameters is much more accurate. Furthermore, fitting the single rupture forces instead of analyzing the gained rupture force distributions (histograms), allows one to check that the theoretical composed distributions, which are based on the extracted parameters in the maximum likelihood estimate, are consistent with the force distributions of the experimental data. A very important finding concerning the choice of the right theoretical model and estimation method was made by the same group in [50]; the statistical uncertainties of the maximum likelihood fit are much smaller than the systematic error generated in models where the consistency check mentioned previously fails.

### Exemplary experiments

Antibodies are of great medical interest with respect to diagnostic and therapeutic applications. In recent years, several groups have investigated antibody–antigen interactions using AFM-based SMFS [12–14,27,52–54]. Morfill *et al.* investigated the interaction between recombinant single-chain Fv antibody fragments and a truncated antigen (12 amino acids long) using AFM-based force spectroscopy, SPR and steered molecular dynamics [53]. For the SMFS experiments, the

single-chain Fv antibody fragment was immobilized on the sample surface covalently via an approximately 45-nm PEG linker. A similar linker attached to the tip was bound to the antigen in three different configurations, termed N-, M- and C-configurations, corresponding to attachment points on the N-terminus, in the middle and on the C-terminus of the antigen (FIGURE 2). While SPR shows that in the absence of external force these variations do not change the dissociation rate, they do change the direction of AFM-applied forces (FIGURE 2), thus yielding significantly different dissociation rates and reaction lengths. AFM cannot explain these differences, but steered molecular dynamics is able to predict the shape of the energy barrier and specify individual bond ruptures. While all configurations bind in the same way, the complex is forced to dissociate via a different pathway due to the external force.

While the dissociation rate from the AFM measurement of configuration C ( $x_b = 1.10 \pm 0.01$  nm;  $k_{\text{off}} = 1.3 [\pm 0.2] \times 10^{-3}\text{s}^{-1}$ ) is close to the one obtained in equilibrium by SPR ( $k_{\text{off}} = 0.9 [\pm 0.2] \times 10^{-3}\text{s}^{-1}$ ), the rate for configuration N is much higher ( $x_b = 0.82 \pm 0.01$  nm;  $k_{\text{off}} = 16.9 [\pm 1.3] \times 10^{-3}\text{s}^{-1}$ ) than the value obtained by SPR ( $k_{\text{off}} = 1.5 [\pm 0.6] \times 10^{-3}\text{s}^{-1}$ ). The errors are calculated based on a cantilever calibration error of 10% and an injected noise and oscillation of  $\pm 0.2$  pN in the measured rupture forces. The main bond of both configurations is the same hydrogen bond. However, if external force is applied, potential walls with greater reaction length are more tilted than those with shorter lengths, thus becoming less important. Due to the difference in pulling direction, N and C are forced to dissociate via different pathways, each with different bonds breaking before the main hydrogen bond. This shows that the multidimensional character of the potential barrier is much more complex, as in the models of FIGURE 3. Furthermore, it demonstrates how sensitive to the immobilization process of the molecules the quantitative results can be, especially for small molecules; for large molecules, the binding site is relatively far away from the attachment point of the linker and so should have less deviation.

Single-molecule force spectroscopy allows for the discrimination and quantitative characterization of different binding modes and sites between two distinct interacting partners. Fuhrmann *et al.* demonstrated the potential of SMFS in this regard by means of a protein–RNA interaction related to post-transcriptional regulation [19]. In this experiment, the RNA target

fragment was attached via a PEG linker to the AFM tip and the protein was coupled covalently to the surface (FIGURE 5A). The authors analyzed the data in accordance with the study by Fuhrmann *et al.* [34]. FIGURE 5C SHOWS a 2D histogram combining rupture forces and rigidity (i.e., the slope before the point of dissociation in the force–distance plot, FIGURE 5B). The complex distribution with multiple peaks indicates different binding modes or sites for the two molecules involved. This was analyzed in

detail in experiments applying different dwell times (i.e., the time the AFM tip rests on the sample surface) and in competition experiments. While the distribution in FIGURE 5C shows a broad, multimodal distribution of forces, the dwell time analysis reveals two distinct peaks. For short dwell times (<210 ms), the analysis results in one peak with a maximum at 60 pN and approximately 6 pN/nm (FIGURE 6A). A second peak at higher force and rigidity (~100 pN and 8 pN/nm) appears (FIGURE 6B). Extending

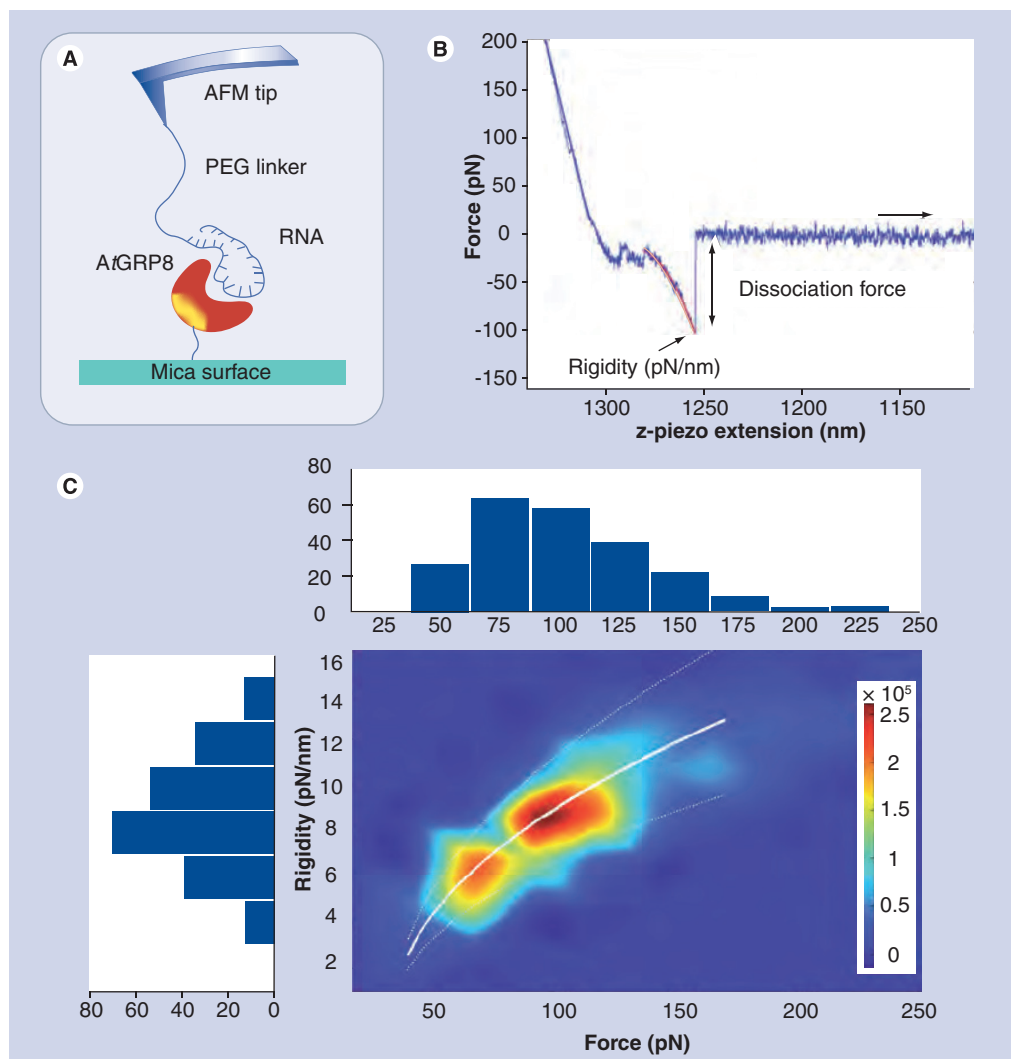


**Figure 5. Protein–RNA interaction.** (A) Schematic illustration of the immobilization of the RNA binding protein and the RNA oligonucleotide. (B) Typical force–distance curve (only the retracting part of the complete force–distance cycle is shown). The nonlinear part of the force–distance curve that precedes the abrupt dissociation event can be fitted by a second degree polynomial (red line). The slope of this polynomial at the point of dissociation is termed rigidity. (C) Data from individual dissociation events (dissociation force, rigidity) of the investigated RNA–protein interaction at a pulling velocity of 5000 nm/s are plotted in a 2D-probability histogram (red: high frequency, blue: low frequency). Projections of the cumulated distributions of the dissociation force and of the rigidity are shown as additional 1D graphs above and left of the 2D-histogram. The white line indicates the corresponding values of rigidity for the master curve and the dashed white lines correspond to the maximum allowed deviation of the rigidity. AFM: Atomic force microscopy; PEG: Poly(ethylene) glycol. Adapted from [19] with permission from Elsevier © (2009).

the dwell time further ( $>330$  ms) results in the low force peak nearly disappearing and the high force peak increasing significantly (FIGURE 6C).

In order to prove that this effect is due to different binding modes or sites, as opposed to an increase of multirupture probability caused by increased dwell times, the authors investigated the influence of competition with free RNA target molecules. It was found that adding the agent results in the disappearance of the peak at higher forces, while the low force peak remains unchanged; similar results were found for the intermediate dwell times where both peaks appear. This indicates that the protein has multiple binding sites with various binding specificities. The application of an improved analysis treatment [34] results in short lifetimes for the nonspecific interactions of approximately 0.5 s and lifetimes of approximately 200 s for the specific interactions.

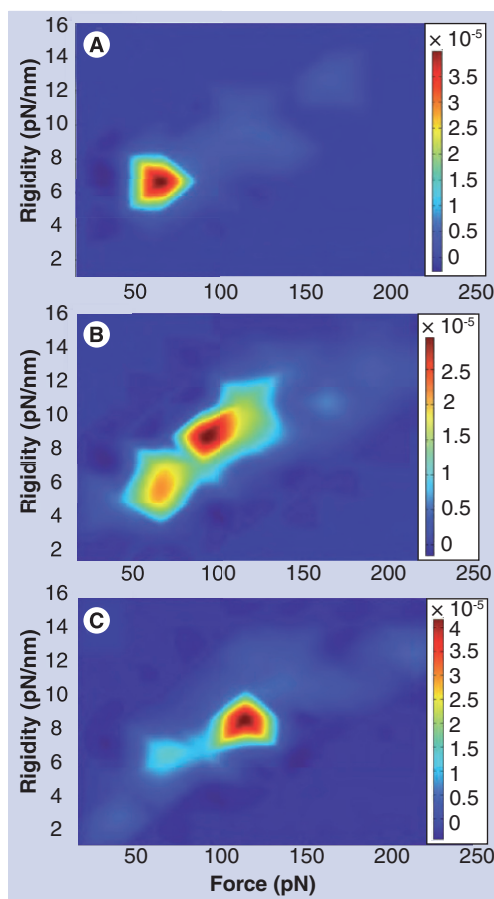


**Figure 6. Dwell time-dependent 2D histograms of the RNA and protein interaction measured at an experimental velocity of 5000 nm/s. (A)** 2D histogram for dwell times of 0.10–0.21 s. **(B)** 2D histogram for dwell times of 0.22–0.32 s. **(C)** 2D histogram for dwell times of 0.33–0.60 s. Adapted from [19] with permission from Elsevier © (2009).

At short dwell times, the RNA is more likely to bind to the rather nonspecific binding sites, while at long dwell times, this low affinity bond can break and the RNA can diffuse and thus find the specific binding site, resulting in a much longer lifetime than the dwell time. It is suggested that this nonspecific binding might also mediate as an intermediated potential barrier, enabling the system to go into the deeper binding by unfolding the RNA loop. In addition, the SMFS experiments give insights into the energy landscape of the interaction between the protein and the corresponding RNA target sequence, resulting in a potential with at least two barriers. The reaction lengths are 0.55 and 0.28 nm for the specific and nonspecific interactions, respectively.

### Conclusion & future perspective

Over the last 15 years, SMFS has been successfully applied to a broad range of ligand–receptor interactions. The sensitivity and the addressable range of affinity constants, along with the advantages of observing the interactions without ensemble averaging, and the low amount of required ligand–receptor molecules for the experiments, together make SMFS a very competitive tool in ligand–receptor research. The reliability and applicability of immobilization procedures of molecules on AFM tips and sample surfaces were significantly improved in recent years and the commercial availability of turnkey AFM systems with force spectroscopy functionality increases research opportunities in the field. These two advances offer biologically and medically oriented laboratories new ways to research ligand–receptor complexes using SMFS.

The analysis of SMFS data sets is still a challenge. At present, significant progress has been made in the automation of the data analysis. In addition, several promising theoretical models were proposed in order to improve the description of the experimental data and to get deeper insights into ligand–receptor interactions. Nevertheless, there is ample room for future improvements. We discussed an example where two different binding modes/sites with different specificity and affinity could be distinguished. This very promising result suggests the application of SMFS to weak multivalent interactions. From a technical point of view, the promise of small cantilevers in commercial atomic force microscopes, and therewith providing a wider dynamic range in SMFS experiments, are finally at hand. Furthermore, several groups are successfully working on the combination of AFM-based SMFS with optical single-molecule fluorescence

spectroscopy techniques, which will facilitate the simultaneous observation of molecular conformational dynamics and ligand–receptor binding processes in future experiments.

### Acknowledgements

The authors acknowledge fruitful discussions and manuscript proofreading of Sebastian Getfert, Bielefeld University, Germany and Jack Staunton, Arizona State University, AZ, USA.

### Financial & competing interests disclosure

Alexander Fuhrmann and Robert Ros are supported by ASU start-up funds and by the NIH grant U54CA143682. The authors have no other relevant affiliations or financial involvement with any organization or entity with a financial interest in or financial conflict with the subject matter or materials discussed in the manuscript apart from those disclosed.

No writing assistance was utilized in the production of this manuscript.

### Executive summary

#### Single-molecule force spectroscopy experiments

- Investigations on single molecules can reveal information about the energy landscape of two binding molecules.
- Single-molecule force spectroscopy has the ability to identify different binding modes and multivalent energy landscapes, hidden in ensemble methods.
- The robust detection and characterization of rupture events in force–distance curves is still challenging and requires fundamental understanding.

#### Theory behind single-molecule force spectroscopy

- The standard theory from Evans & Ritchie is still commonly used.
- Several modifications to the standard theory have tried to improve the agreement between experiment and theory.
- Disagreement between experimental data and theoretical models not fully understood.

#### Exemplary experiments

- A feasibility experiment demonstrates the sensitivity of the quantitative results to the experimental design.
- The exemplary experiment of a protein–RNA binding system demonstrates the advantages of measuring interactions on the single-molecule level.

### Bibliography

Papers of special note have been highlighted as:

- of interest

- 1 Gopalakrishnan M, Forsten-Williams K, Cassino TR, Padro L, Ryan TE, Taeuber UC: Ligand rebinding: self-consistent mean-field theory and numerical simulations applied to surface plasmon resonance studies. *Eur. Biophys. J.* 34(7), 943–958 (2005).
- 2 Bustamante C, Macosko JC, Wuite GJ: Grabbing the cat by the tail: manipulating molecules one by one. *Nat. Rev. Mol. Cell Biol.* 1, 130–136 (2000).
- Excellent review of mechanical single-molecule methods.
- 3 Joo C, Balci H, Ishitsuka Y, Buranachai C, Ha T: Advances in single-molecule fluorescence methods for molecular biology. *Annu. Rev. Biochem.* 77, 51–76 (2008).
- 4 Goesch M, Rigler R: Fluorescence correlation spectroscopy of molecular motions and kinetics. *Adv. Drug Deliv. Rev.* 57(1), 169–190 (2005).
- 5 Binnig G, Quate CF, Gerber C: Atomic force microscope. *Phys. Rev. Lett.* 56(9), 930–933 (1986).
- 6 Meyer G, Amer NM: Novel optical approach to atomic force microscopy. *Appl. Phys. Lett.* 53(12), 1045–1047 (1988).
- 7 Ralston J, Larson I, Rutland MW, Feiler AA, Kleijn M: Atomic force microscopy and direct surface force measurements. *Pure Appl. Chem* 77(12), 2149–2170 (2005).
- 8 Lee GU, Chrisey LA, Colton RJ: Direct measurement of the forces between complementary strands of DNA. *Science* 266, 771–773 (1994).
- 9 Florin EL, Moy VT, Gaub HE: Adhesion forces between individual ligand–receptor pairs. *Science* 264, 415–417 (1994).
- 10 Lee GU, Kidwell DA, Colton RJ: Sensing discrete streptavidin–biotin interactions with atomic force microscopy. *Langmuir* 10(2), 354–357 (1994).
- 11 Dammer U, Popescu O, Wagner P, Anselmetti D, Güntherodt HJ, Misevic GN: Binding strength between cell adhesion proteoglycans measured by atomic force microscopy. *Science* 267, 1173–1175 (1995).
- 12 Allen S, Chen X, Davies J *et al.*: Detection of antigen–antibody binding events with atomic force microscope. *Biochemistry* 36, 7457–7463 (1997).
- 13 Hinterdorfer P, Baumgartner W, Gruber H, Schilcher K, Schindler H: Detection and localization of individual antibody–antigen recognition events by atomic force microscopy. *Proc. Natl Acad. Sci. USA* 93, 3477–3481 (1996).
- 14 Morfill J, Blank K, Zahnd C *et al.*: Affinity-matured recombinant antibody fragments analyzed by single-molecule force spectroscopy. *Biophys. J.* 93(10), 3583–3590 (2007).
- 15 Bartels FW, Mcintosh M, Fuhrmann A *et al.*: Effector-stimulated single molecule protein–DNA interactions of a quorum-sensing system in *Sinorhizobium meliloti*. *Biophys. J.* 92(12), 4391–4400 (2007).
- 16 Baumgarth B, Bartels FW, Anselmetti D, Becker A, Ros R: Detailed studies of the binding mechanism of the *sinorhizobium meliloti* transcriptional activator expg to DNA. *Microbiology-Sgm* 151, 259–268 (2005).
- 17 Kuhner F, Costa LT, Bisch PM, Thalhammer S, Heckl WM, Gaub HE: Lexa–DNA bond strength by single molecule force spectroscopy. *Biophys. J.* 87(4), 2683–2690 (2004).
- 18 Bartels FW, Baumgarth B, Anselmetti D, Ros R, Becker A: Specific binding of the regulatory protein expg to promoter regions of the galactoglucan biosynthesis gene cluster of *Sinorhizobium meliloti* – a combined molecular biology and force spectroscopy investigation. *J. Struct. Biol.* 143, 145–152 (2003).
- 19 Fuhrmann A, Schoning J, Anselmetti D, Staiger D, Ros R: Quantitative analysis of single molecule RNA–protein interaction. *Biophys. J.* 96(12), 5030–5039 (2009).
- 20 Lynch S, Baker H, Byker S, Zhou D, Sinniah K: Single molecule force spectroscopy of guanine quadruplex DNA. *Biophys. J.* 96(3S1), 36–36 (2009).
- 21 Porter-Peden L, Kamper SG, Wal MV, Blankespoor R, Sinniah K: Estimating kinetic and thermodynamic parameters from single molecule enzyme inhibitor interactions. *Langmuir* 24(20), 11556–11561 (2008).

- 22 Fritz J, Katopodis AG, Kolbinger F, Anselmetti D: Force-mediated kinetics of single p-selectin/ligand complexes observed by atomic force microscopy. *Proc. Natl Acad. Sci. USA* 95, 12283–12288 (1998).
- 23 Bucior I, Garcia-Manyes S, Ros R *et al.*: Strong specific binding forces between adhesive extracellular proteoglycan carbohydrates. *FEBS J.* 272, 340–340 (2005).
- 24 Bjoernham O, Schedin S: Methods and estimations of uncertainties in single-molecule dynamic force spectroscopy. *Eur. Biophys. J.* 38(7), 911–922 (2009).
- 25 Eckel R, Wilking SD, Becker A, Sewald N, Ros R, Anselmetti D: Single molecule experiments in synthetic biology – a new approach for the affinity ranking of DNA-binding peptides. *Angew. Chem. Int. Ed.* 44, 3921–3924 (2005).
- 26 Eckel R, Ros R, Decker B, Mattay J, Anselmetti D: Supramolecular chemistry at the single molecule level. *Angew. Chem. Int. Ed.* 44, 484–488 (2005).
- 27 Schwesinger F, Ros R, Strunz T *et al.*: Unbinding forces of single antibody–antigen complexes correlate with their thermal dissociation rates. *Proc. Natl Acad. Sci. USA* 97(18), 9972–9977 (2000).
- 28 Hinterdorfer P, Dufřine YF: Detection and localization of single molecular recognition events using atomic force microscopy. *Nat. Methods* 3(5), 347–355 (2006).
- Nice review about atomic force microscopy-based single-molecule force spectroscopy.
- 29 Evans E, Ritchie K: Dynamic strength of molecular adhesion bonds. *Biophys. J.* 72(4), 1541–1555 (1997).
- Although the theoretical models have been improved a couple of times, this is still the main work for the quantitative description of ligand–receptor force spectroscopy.
- 30 Janovjak H, Struckmeier J, Mueller D: Hydrodynamic effects in fast AFM single-molecule force measurements. *Eur. Biophys. J.* 34(1), 91–96 (2005).
- 31 Dudko OK, Hummer G, Szabo A: Theory, analysis, and interpretation of single-molecule force spectroscopy experiments. *Proc. Natl Acad. Sci. USA* 105(41), 15755 (2008).
- Provides an easy method to analyze the data with extended Bell models, without the need of computer-based least square fits.
- 32 Levy R, Maaloum M: New tools for force spectroscopy. *Ultramicroscopy* 102(4), 311–315 (2005).
- 33 Odorico M, Teulon JM, Berthoumieu O, Chen SW, Parot P, Pellequer JL: An integrated methodology for data processing in dynamic force spectroscopy of ligand–receptor-binding. *Ultramicroscopy* 107(10–11), 887–894 (2007).
- 34 Fuhrmann A, Anselmetti D, Ros R, Getfert S, Reimann P: Refined procedure of evaluating experimental single-molecule force spectroscopy data. *Physical Rev. E* 77(3), 31912 (2008).
- Demonstrates how careful force curve analysis can be carried out by using automated algorithms.
- 35 Carl P, Kwok CH, Manderson G, Speicher DW, Discher DE: Forced unfolding modulated by disulfide bonds in the Ig domains of a cell adhesion molecule. *Proc. Natl Acad. Sci. USA* 98(4), 1565 (2001).
- 36 Gergely C, Senger B, Voegel JC, Hoerber JK, Schaaf P, Hemmerle J: Semi-automatized processing of AFM force-spectroscopy data. *Ultramicroscopy* 87(1–2), 67 (2001).
- 37 Bosshart Pd, Casagrande F, Frederix P *et al.*: High-throughput single-molecule force spectroscopy for membrane proteins. *Nanotechnology* 19, 384014 (2008).
- 38 Bell GI: Models for the specific adhesion of cells to cells. *Science* 200(4342), 618 (1978).
- 39 Friedsam C, Wehle AK, Kuhner F, Gaub HE: Dynamic single-molecule force spectroscopy: bond rupture analysis with variable spacer length. *J. Phys. Condens. Matter* 15(18), 1709–1724 (2003).
- 40 Ray C, Brown Jr, Akhremitchev BB: Correction of systematic errors in single-molecule force spectroscopy with polymeric tethers by atomic force microscopy. *J. Phys. Chem. B* 111(8), 1963–1974 (2007).
- 41 Thormann E, Hansen PL, Simonsen AC, Mouritsen OG: Dynamic force spectroscopy on soft molecular systems: improved analysis of unbinding spectra with varying linker compliance. *Colloids Surf. B Biointerfaces* 53(2), 149–156 (2006).
- 42 Raible M, Evstigneev M, Reimann P, Bartels FW, Ros R: Theoretical analysis of dynamic force spectroscopy experiments on ligand–receptor complexes. *J. Biotechnol.* 112(1–2), 13–23 (2004).
- 43 Evstigneev M, Reimann P: Dynamic force spectroscopy: optimized data analysis. *Physical Rev. E* 68(4), 45103 (2003).
- 44 Gu C, Kirkpatrick A, Ray C, Guo S, Akhremitchev BB: Effects of multiple-bond ruptures in force spectroscopy measurements of interactions between fullerene C60 molecules in water. *J. Phys. Chem. C* 112(13), 5085–5092 (2008).
- 45 Guo S, Ray C, Kirkpatrick A, Lad N, Akhremitchev BB: Effects of multiple-bond ruptures on kinetic parameters extracted from force spectroscopy measurements: revisiting biotin–streptavidin interactions. *Biophys. J.* 95(8), 3964–3976 (2008).
- Detailed analysis of the influence of double rupture events.
- 46 Sulchek T, Friddle R, Ratto T, Albrecht H, Denardo S, Noy A: Single-molecule approach to understanding multivalent binding kinetics. *Ann. NY Acad. Sci.* 1161, 74–82 (2009).
- 47 Raible M, Evstigneev M, Bartels FW *et al.*: Theoretical analysis of single-molecule force spectroscopy experiments: heterogeneity of chemical bonds. *Biophys. J.* 90(11), 3851–3864 (2006).
- Introduces the heterogeneity of bond model.
- 48 Merkel R, Nassoy P, Leung A, Ritchie K, Evans E: Energy landscapes of receptor–ligand bonds explored with dynamic force spectroscopy. *Nature* 397(6714), 50–53 (1999).
- 49 Dudko OK, Hummer G, Szabo A: Intrinsic rates and activation free energies from single-molecule pulling experiments. *Phys. Rev. Lett.* 96(10), 108101 (2006).
- 50 Getfert S, Evstigneev M, Reimann P: Single-molecule force spectroscopy: practical limitations beyond bellis model. *Physica A* 388(7), 1120–1132 (2009).
- Gives an excellent insight to the problems of analyzing single-molecule force spectroscopy ligand–receptor data.
- 51 Getfert S, Reimann P: Optimal evaluation of single-molecule force spectroscopy experiments. *Physical Rev. E* 76(5), 52901 (2007).
- 52 Dammer U, Hegner M, Anselmetti D *et al.*: Specific antigen/antibody interactions measured by force microscopy. *Biophys. J.* 70, 2437–2441 (1996).
- 53 Morfill J, Neumann J, Blank K *et al.*: Force-based analysis of multidimensional energy landscapes: application of dynamic force spectroscopy and steered molecular dynamics simulations to an antibody fragment–peptide complex. *J. Molec. Biol.* 381(5), 1253–1266 (2008).
- A very detailed analysis of the reliability of single-molecule force spectroscopy ligand–receptor experiments.
- 54 Ros R, Schwesinger F, Anselmetti D *et al.*: Antigen binding forces of individually addressed single-chain fv antibody molecules. *Proc. Natl Acad. Sci. USA* 95, 7402–7405 (1998).